

Optical Waveguides with Embedded Air-gap Cladding Integrated Within a Sea-of-Leads (SoL) Wafer-level Package

[†]Anthony Mule', [†]Muhannad Bakir, [†]Joseph Jayachandran, [†]Ricardo Villalaz, [†]Hollie Reed, ^{††}Navnit Agrawal, ^{††}Shom Ponoht, ^{††}Joel Plawsky, ^{††}Peter Persans, [†]Paul Kohl, [†]Kevin Martin, [†]Elias Glytsis, [†]Thomas Gaylord, and [†]James Meindl

[†]Georgia Institute of Technology, Atlanta, GA 30332-0269, Email: tvmmule@ieee.org

^{††}Rensselaer Polytechnic Institute, Troy, NY 12180-3590, Email: persap@rpi.edu

Abstract

Optical waveguides are integrated into a Sea-of-Leads (SoL) wafer-level package. A photo-sensitive polycarbonate composite is incorporated to provide a buried air-gap cladding that allows a refractive index contrast, Δn , between waveguide core and cladding regions of $\Delta n = 0.52$. The final package contains 1000 electrical input/output (I/O) interconnects and 32 large-area optical waveguides for electrical chip-to-chip and optical intra-chip clock or data interconnection, respectively. Monolithic fabrication of passive optical interconnect components is described.

Introduction

Wafer-level batch packaging is currently under investigation to address the high power, I/O density, and I/O bandwidth requirements of future technology generations [1,2]. The 2001 International Technology Roadmap for Semiconductors (ITRS) projects that 22 nm (year 2016) high performance microprocessors will dissipate 288 W from a 0.4 V power supply [2]. This translates into the need for 720 A of current to be delivered through the chip package¹. Total pin count and cost per pin are projected to be 1318-4702 and 0.36-0.79 cents/pin for cost-performance applications, implying the need for very low cost in the provision of high pin-count packaging.

A potential solution identified by the ITRS to the performance limitations introduced by global electrical interconnects is the use of optical interconnections [2]. Optical waveguides allow for planar packaging of a hybrid electrical/optical system in a manner conducive to the delivery of future heat removal and power supply requirements. In addition, polymer waveguide technologies offer immediate, low-cost compatibility with wafer-level fabrication processes.

Figure 1 illustrates a SoL package integrating optical waveguide interconnection. As depicted in

Fig. 1, optical power will be coupled into the wafer-level package from an off-chip source through volume grating couplers [4]. The integration of volume couplers within the package allows for the mitigation of alignment concerns with respect to board-to-package and package-to-chip coupling, as a) input couplers can be sized to cover the range of expected deviations in input beam location in a manner free from via blockage concerns, and b) exact placement of output couplers above chip-level detectors is possible. The inclusion of embedded air-gap regions allows for a significant increase in Δn and hence permits smaller bending radii and higher waveguide densities. An additional advantage of placing optical waveguides within the package is the elimination of via blockage concerns with respect to waveguide routing. Finally, wafer-level package integration allows for high-volume in-situ testing of intra-chip optical interconnection.

In this paper, optical waveguides with an embedded air-gap cladding region are integrated within a compliant wafer-level package. The results presented here include the fabrication of package-level guided-wave interconnection and air-gap cladding regions. Integration issues associated with volume grating technology are also discussed.

Fabrication

Figure 2 illustrates the general fabrication sequence with respect to waveguide incorporation. The process begins by defining bond pad regions atop a 1.8 μm layer of PECVD SiO_2 (Figure 2a). The SiO_2 serves as both passivation for underlying circuitry and the lower cladding for optical waveguides. Preparation of the SiO_2 surface for waveguide application is performed by applying hexamethyldisilazane (HMDS) primer. A UV curable alkoxy-siloxane epoxy [5] waveguide material obtained from Polyset Inc. is spun onto the sample at a thickness of 1.2 μm (Figure 2b). A 5.1 J/cm^2 blanket exposure and 1.5 hr oven bake at 150° C are performed to cure the waveguide layer. For this

¹ Assuming no DC-to-DC conversion is employed [3].

experiment, 50 μm -wide channel waveguide regions were defined via reactive ion etching with an 8:1 O_2/CHF_3 plasma created at 300 W power and 5 mT pressure. Approximately 0.8 μm of the 1.2 μm core region was etched to leave a rib waveguide geometry (Figure 2c). Next, 4-5 μm of a sacrificial photosensitive polycarbonate composite (Unity 200) is applied to create embedded air-gap regions (Figure 2d). The sacrificial layer is patterned with a 1 J/cm^2 dose of 240 nm radiation to initiate decomposition within the exposed regions. Complete decomposition occurs during a subsequent 2 min 110°C soft bake (Figure 2e). A 3-4 μm layer of Avatrel polymer is then applied as an overcoat (Figure 2f). Finally, the sample is cured at 160°C for 4 hr, during which time the remaining polycarbonate regions decompose to leave an embedded air-gap (Figure 2g).

Results

A portion of the 1000 electrical I/Os and 32 optical waveguides is shown in Fig. 3. A micrograph of a single waveguide is given in Fig. 4 where a) individual compliant leads, b) an optical waveguide, and c) a buried air-gap region are shown. Figure 5 illustrates an SEM cross-section of a waveguide/air-gap region, illustrating successful decomposition and curing of the air-gap and overcoat materials. By incorporating a buried air-gap, a $\Delta n = 0.52$ is achieved between core and cladding regions.

Volume grating coupler integration within a SoL package begins with the realization of a large-area (or slab) grating consisting of appropriate waveguide and grating materials. To this end, a slab volume grating coupler has been fabricated using the epoxy waveguide material and a holographic photopolymer available from Dupont [6]. Fabrication of the volume coupler begins with the deposition of an approximately 0.9 μm thick waveguide layer atop a fused-silica substrate prepared with HMDS primer, where the refractive index of the fused silica substrate is approximately the same as that of the SiO_2 passivation layer. After a soft bake, a second layer of HMDS is applied, after which the waveguide sample and a pre-exposed laminate sheet of photopolymer are rinsed in isopropanol, dried with a N_2 gun, and laminated together using a hand roller. Exposure of the laminate sheet prior to waveguide application proceeds in the same manner as that in [4]. After a 15 min wait period, a back-side Mylar sheet that serves to package the laminate photopolymer is removed, whereby the sample is subjected to a 150 mJ/cm^2 blanket dose

of UV radiation to lock the holographic grating profile and cured at 150°C for 2 hrs.

Measurements of transmitted intensity vs. incident angle are provided for the slab coupler in Fig. 6. To test the Bragg angle of a fabricated coupler, the sample is mounted onto a rotation stage, where a 632 nm HeNe test beam passes through the sample directly into a detector. The sample is rotated until a dip in transmitted intensity is observed. This dip occurs due to the coupling of optical power into the waveguide region away from the detector. Figure 6 illustrates the test results corresponding to a volume grating coupler with a Bragg angle of approximately 35°.

Volume couplers achieving Bragg angles of 0° are currently under investigation for surface-normal coupling. Following the realization of a surface-normal slab coupler, integration of volume grating technology will proceed with the transformation of functional slab gratings into multiple channel waveguides, where each waveguide channel will link two separate input and output grating regions. Future versions of the technology will incorporate smaller waveguide geometries than those of the present sample. Once channel waveguides with volume couplers have been realized, package-level integration will be performed.

Acknowledgements

This work is supported by the Semiconductor Research Corporation (Contract SJ-374).

References

- [1] A. Naeemi et al., *Proc. IEEE International Solid State Circuits Conference*. San Francisco, CA: pp., 280-281, Feb. 2001.
- [2] International Technology Roadmap for Semiconductors, 2001 update.
- [3] S-J Jou and T-L Chen, *IEEE J. Solid-State Circuits*, vol. 45, pp. 617-625, May 1998.
- [4] S. M. Schultz, E. N. Glytsis, and T. K. Gaylord, *Opt. Lett.*, vol. 24, pp. 1708-1710, Dec. 1999.
- [5] A. Jain et al., *Thin Solid Films*, vol. 398-399, pp. 513-522, 2001.
- [6] J. Yeh, A. Harton, and K. Wyatt, *Appl. Opt.*, vol. 37, pp. 6270-6274, Sept. 1998.

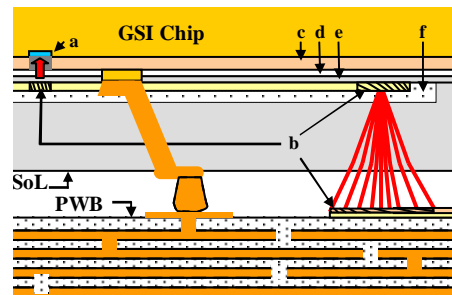


Figure 1: Proposed structure. Labeled are a) detector, b) grating coupler layer, c) CMOS metallization, d) passivation, e) waveguide core, and f) embedded air-gap.

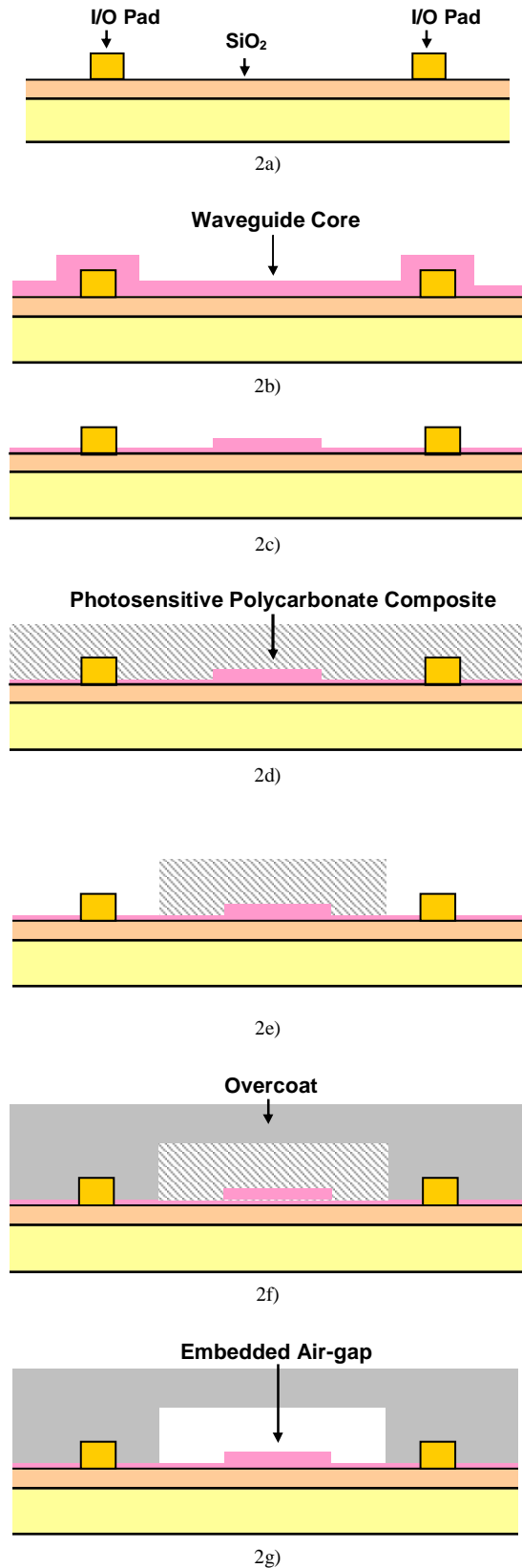


Figure 2: Waveguide fabrication flow.

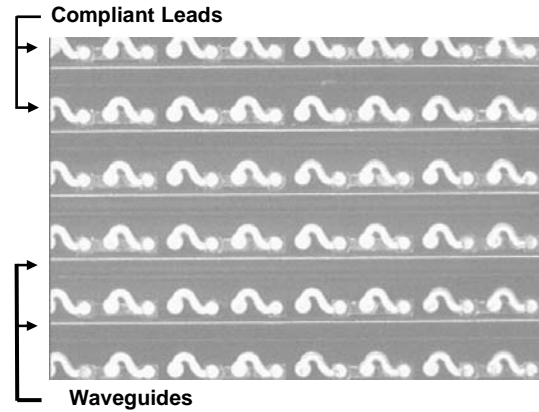


Figure 3: Array of leads and waveguides.

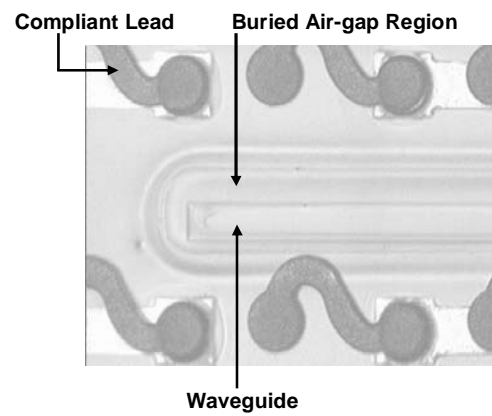


Figure 4: Micrograph of waveguide, air-gap regions.

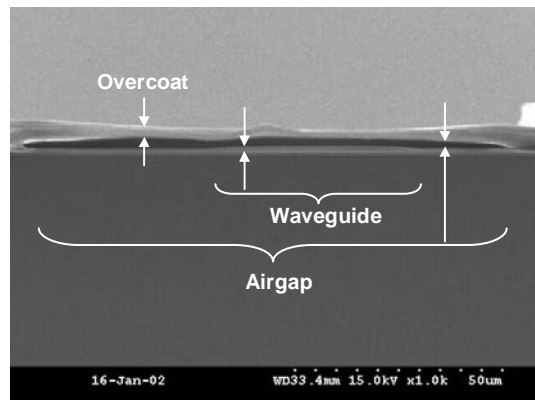


Figure 5: SEM cross-section of waveguide, air-gap regions.

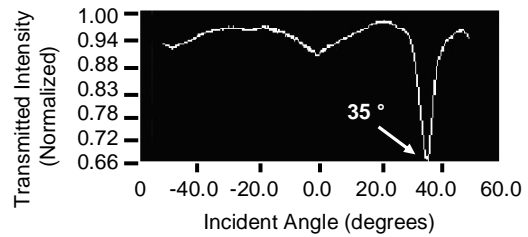


Figure 6: Transmitted intensity vs. incident angle measurements of volume grating coupler.

